The Astrophysical Journal, 684:626–634, 2008 September 1
© 2008. The American Astronomical Society. All rights reserved. Printed in U.S.A.

^{3}He-DRIVEN MIXING IN LOW-MASS RED GIANTS: CONVECTIVE INSTABILITY IN RADIATIVE AND ADIABATIC LIMITS

Pavel A. Denissenkov[1,2] and Marc Pinsonneault[1]
Received 2007 March 13; accepted 2008 May 14

ABSTRACT

We examine the stability and observational consequences of mixing induced by ^{3}He burning in the envelopes of first ascent red giants. We demonstrate that there are two unstable modes: a rapid, nearly adiabatic mode that we cannot identify with an underlying physical mechanism, and a slow, nearly radiative mode that can be identified with thermohaline convection. We present observational constraints that make the operation of the rapid mode unlikely to occur in real stars. Thermohaline convection turns out to be fast enough only if fluid elements have fingerlike structures with a length-to-diameter ratio $l/d \gtrsim 10$. We identify some potentially serious obstacles for thermohaline convection as the predominant mixing mechanism for giants. We show that rotation-induced horizontal turbulent diffusion may suppress the ^{3}He-driven thermohaline convection. Another potentially serious problem for it is to explain observational evidence of enhanced extra mixing. The ^{3}He exhaustion in stars approaching the red giant branch (RGB) tip should make the ^{3}He mixing inefficient on the asymptotic giant branch (AGB). In spite of this, there are observational data indicating the presence of extra mixing in low-mass AGB stars similar to that operating on the RGB. Overmixing may also occur in carbon-enhanced metal-poor stars.

Subject headings: stars: abundances — stars: evolution — stars: interiors

1. INTRODUCTION

There is strong observational evidence for deep mixing in the radiative envelopes of low-mass ($M \lesssim 2\ M_\odot$) red giant branch (hereafter, LM-RGB) stars. Changes in light-element abundances (such as Li, C, N) and in the ^{12}C/^{13}C ratio as a function of luminosity have been seen in low- and solar-metallicity red giants both in the field and in stellar clusters (e.g., Gilroy & Brown 1991; Gratton et al. 2000; Bellman et al. 2001; Keller et al. 2001; Grundahl et al. 2002; Shetrone 2003; Smith & Martell 2003; Smith & Briley 2006; Spite et al. 2006). The observed pattern requires at least a component of in situ mixing. This extra mixing could have consequences for other species (such as ^{3}He) that are not directly observed. Indeed, in spite of the predicted efficient production of ^{3}He in low-mass main-sequence (MS) stars, its Galactic abundance has been nearly constant since the epoch of big bang nucleosynthesis (e.g., Tosi 1998; Bania et al. 2002; Vangioni et al. 2003). To explain this, semiempirical stellar evolution models have shown that the carbon depletion due to extra mixing in LM-RGB stars should unavoidably be accompanied by a strong ^{3}He destruction that counterbalances its production on the MS (Rood et al. 1984; Hogan 1995; Charbonnel 1995; Weiss et al. 1996).

However, the true physical process that is responsible for mixing has resisted identification. Rotationally induced mixing has been an implied underlying mechanism since the pioneering work of Sweigart & Mengel (1979), but there are serious difficulties in reconciling the observed mixing pattern with theoretical predictions (Chanamé et al. 2005; Palacios et al. 2006). Moreover, it can be shown that rotational mixing solely dependent on the local angular velocity gradient $q \equiv (\partial \ln \Omega/\partial \ln r)$ (e.g., shear mixing) will be self-quenching. Indeed, the empirically constrained mixing rate $v_{\rm mix} \gtrsim 10^{-3}$ to 10^{-2} cm s^{-1} (see § 5) is faster (as it should be) than the mass inflow rate $|\dot{r}| \leq 10^{-4}$ cm s^{-1} in the radiative zones of LM-RGB stars. Hence, if $v_{\rm mix}$ were proportional to $|q|^n$ ($n > 0$), then the flattening of the rotation profile by the accompanying angular momentum redistribution would quench the mixing very quickly.

A very different class of solution has recently been proposed by Eggleton et al. (2006, hereafter EDL06; see also Eggleton et al. 2007). While investigating the core He flash in a low-mass model star near the RGB tip with the code Djehuty,[3] Dearborn et al. (2006) noticed some gas motions in the radiative zone above the H-burning shell, in addition to convective motions driven by ^{4}He burning in the core. In their follow-up papers, they have made the conclusion that these additional gas motions are due to the Rayleigh-Taylor instability (RTI) driven by ^{3}He burning. They have noted that, unlike other nuclear reactions in stars, the reaction ^{3}He (^{3}He, $2p$)^{4}He decreases the mean molecular weight μ. EDL06 have argued that, even though the decrease of μ is minute ($|\Delta\mu| \sim 10^{-4}$), it is the resulting local inversion of the μ-gradient $\nabla_\mu \equiv (d \ln \mu/d \ln P) < 0$ that has led to the RTI in their three-dimensional (3D) simulations. They claim that velocities of gas motions induced by the RTI are "comparable to the velocity of the normal convection" ($v_c \sim 10^5$ cm s^{-1}) and that this is consistent with the simple heuristic estimate of $v^2 \sim gH_P(\Delta\mu/\mu)$, where g and H_P are the local gravity and pressure scale height, respectively.

A μ-gradient inversion from ^{3}He burning is a predicted consequence of standard stellar evolution. After a low-mass star has left the MS, its convective envelope first deepens (the first dredge-up) and then its bottom starts to recede. At the depth of its maximum inward penetration the convective envelope imprints a discontinuity in the chemical composition profile. Later on, the advancing in the mass H-burning shell will erase this discontinuity. During this event the evolution of the star slows

[1] Department of Astronomy, Ohio State University, 4055 McPherson Laboratory, 140 West 18th Avenue, Columbus, OH 43210; dpa@astronomy.ohio-state.edu, pinsono@astronomy.ohio-state.edu.
[2] On leave from Sobolev Astronomical Institute of St. Petersburg State University, Universitetsky Prospekt 28, Petrodvorets, 198504 St. Petersburg, Russia.

[3] This is a 3D explicit hydrodynamics code with the time step constrained by the Courant condition which can couple to a 1D stellar evolution code.

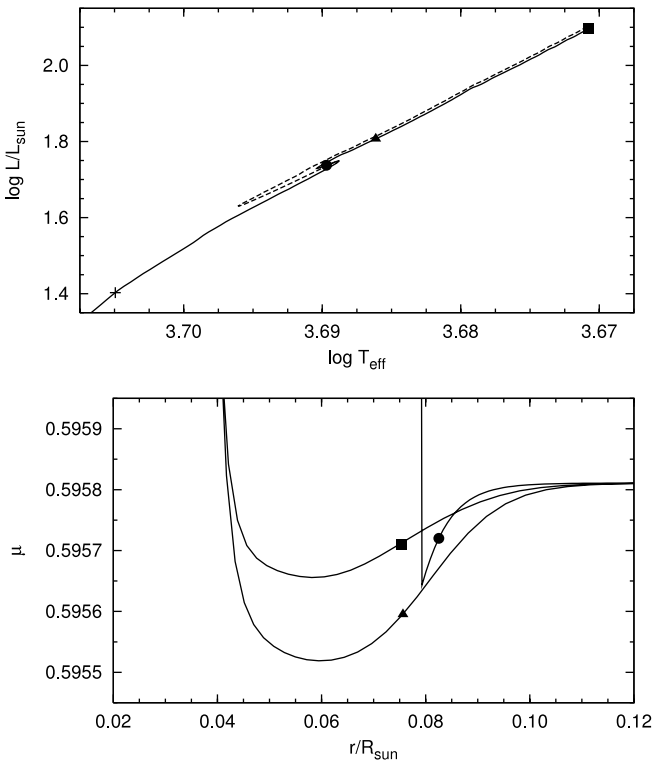

FIG. 1.—*Top*: Evolutionary tracks of a 0.83 $M_\odot$ model star (the initial H and He mass fractions are $X = 0.758$ and $Y = 0.24$) near the bump luminosity (the solid curve is for $\Gamma = 0.01$; the dashed curve is for $\Gamma = 0.4$). Cross marks the end of the first dredge-up. *Bottom*: Profiles of the mean molecular weight in the radiative zones of our unmixed red giant models, locations of which are shown with the same symbols in the top panel. Depressions of μ are caused by the reaction ^{3}He (^{3}He, $2p$)^{4}He.

down, which produces bumps in differential luminosity functions of stellar clusters, and the star itself makes a tiny zigzag on the H-R diagram (Fig. 1, *top*). However, before the major H-burning shell erases the composition discontinuity, a shell in which ^{3}He burns down and which advances in front of the H-burning shell will cross the discontinuity first. The ^{3}He(^{3}He,$2p$)^{4}He reaction reduces the mean molecular weight locally. However, this reduction is so minute, $\Delta\mu \approx \mu^2 \Delta X_3/6 \approx -10^{-4}$ (here, $\mu \approx 0.6$, and X_3 is the ^{3}He mass fraction that can reach up to a value of $\sim 2 \times 10^{-3}$ in the envelope of a low-mass star ascending the RGB), that it is not seen on the μ-profile until the μ-depression finds itself in the chemically homogeneous region of the radiative zone previously occupied by the convective envelope. This happens close to the bump luminosity (Fig. 1).

In this paper we investigate the ^{3}He instability in more detail. First of all, we note that the RTI would not be expected in compressible, and hence stratified, stellar material. However, a μ-gradient inversion may trigger instabilities related to convection. In § 2 we discuss general criteria for convective instability, taking into consideration that, over longer timescales, fluid elements can exchange heat with their surroundings, thus modifying the background temperature stratification. We identify two families of solutions: a rapid mode with a nearly adiabatic thermal structure and a slow mode with a nearly radiative structure. The EDL06 results appear to correspond to the rapid mode, while the slow mode can be identified as thermohaline convection (e.g., Vauclair 2004). On the basis of previously published diffusion coefficient estimates, it is likely to be triggered in the envelopes of red giants. However, there are significant (and uncertain) assumptions related to the actual operation of this instability. We discuss key features determining the efficiency of the slow mode: the assumed geometry of the fluid elements, which directly impacts the timescale for exchanging heat; the potential impact of horizontal turbulence in suppressing the instability; and the predicted depth of mixing. In § 3 we demonstrate that the alternative approach based on the linear stability analysis of the underlying conservation equations also leads to the conclusion that thermohaline convection may be suppressed by the horizontal turbulent diffusion.

In § 4 we evaluate the impact of any proposed mixing mechanism on the thermal structure of the red giant branch stars. We argue that the rapid mode, which is similar in its properties to the originally published results of EDL06, can be ruled out, because it would induce strong feedback on the thermal structure of giants and would predict a mixing pattern contrary to observations. We also demonstrate that both the slow mode and prior empirical mixing estimates would not disturb the thermal structure of giants. In § 4 we assess the overall promise of ^{3}He mixing as a mechanism. We find that it may be an attractive solution, but identify several potentially serious drawbacks on both observational and theoretical grounds. In particular, we argue that previously published estimates of horizontal turbulence would be sufficient to suppress the instability and that the naturally expected depth of mixing and trends with luminosity may be in conflict with observational trends.

2. GENERAL CRITERIA FOR CONVECTIVE INSTABILITY

In the presence of a positive μ-gradient $d\mu/dr$ (a negative ∇_μ), a fluid element displaced vertically upward will find itself surrounded by material with a higher μ. Whether the fluid element will continue to rise depends on how efficiently it can exchange mass and heat with its surroundings. It is easy to anticipate that heat diffusion will favor the instability by reducing the temperature gradient inside the rising fluid element $\nabla' \equiv (d \ln T'/d \ln P)$, as compared to its adiabatic value $\nabla_{\rm ad}$, and slightly increasing the gradient in the surrounding medium $\nabla \equiv (d \ln T/d \ln P)$, as compared to its radiative value $\nabla_{\rm rad}$ in the absence of mixing. In a radiative zone, we always have $\nabla_{\rm rad} \leq \nabla < \nabla' < \nabla_{\rm ad}$. On the other hand, molecular diffusion and horizontal turbulent diffusion (if the latter is present it will also contribute to heat diffusion) will decrease the μ-contrast between the fluid element and its surroundings $|\Delta\mu| = |\mu'(r) - \mu(r)|$, thus hindering the development of convection. Current theories of rotational mixing predict the existence of strong horizontal turbulence (Chaboyer & Zahn 1992; Maeder 2003; Mathis et al. 2004); even if the vertical turbulence is not strong enough to produce mixing, such a horizontal turbulence could strongly impact an instability driven by differences in composition. Let us carry out a general investigation of effects produced by these diffusion processes on the convective instability of the radiative zone in the presence of a μ-gradient inversion. The magnitude of these effects depends on the Péclet number that represents a ratio of thermal and mixing timescales

$$\mathrm{Pe} = \frac{\tau_{\rm th}}{\tau_{\rm mix}} \approx \frac{lv}{(K + D_h)} \left(\frac{d}{l}\right)^2,$$

where $\tau_{\rm th} \approx d^2/(K + D_h)$ and $\tau_{\rm mix} \approx l/v$. Here, we consider the possibility that the convective motions may be organized in elongated narrow structures resembling "fingers" whose length l is much larger than their diameter d. In this case, the fluid element velocity v, thermal diffusivity K, and horizontal turbulent diffusivity D_h should appropriately be averaged over the finger length

scale l. For simplicity, we represent a "finger" by a spherical fluid element of the diameter d that travels the path $l \geq d$ before it dissolves. Modeling a "finger" with a cylinder would introduce factors of order unity in our derived relations. In the limit of a high Péclet number, mixing is so fast compared to heat exchange that T' undergoes nearly adiabatic changes, hence $\nabla' \approx \nabla_{\rm ad}$. In this limit, when the rising fluid element dissolves it has a lower temperature than its surroundings; therefore, it reduces T locally, making ∇ steeper and closer to $\nabla_{\rm ad}$. In the opposite limit of a low Péclet number, mixing is so slow that the radiative and turbulent heat flux from the surroundings can warm up the fluid element thoroughly as it rises. This brings ∇' close to $\nabla_{\rm rad}$, while ∇ remains nearly equal to $\nabla_{\rm rad}$, because the fluid element will have $T' \approx T$ when it dissolves.

In our further analysis we use simple heuristic relations obtained in the mixing length approximation by Maeder (1995) and Talon & Zahn (1997) in their investigations of shear instabilities in rotating stars. We admit that the radiative zone may host both the ^{3}He-driven convection and some other extra mixing of a nonconvective origin (e.g., rotation-driven turbulent diffusion or meridional circulation) at the same time. Following Zahn (1992), we assume that rotation-driven turbulence is highly anisotropic, with horizontal components of the turbulent viscosity strongly dominating over those in the vertical direction, $D_h \gg D_v$. We consider a process with a diffusion coefficient $D_{\rm mix} = vl/3$. At the present stage we leave $D_{\rm mix}$ unspecified and simply solve for the coupled diffusion of heat and chemicals to evaluate the range of diffusion coefficients over which an instability occurs. In § 4 we compare with specific (and previously published) estimates of diffusion coefficients.

The degree to which convection modifies the thermal structure of the radiative zone depends on its heat transport efficiency

$$\Gamma = \frac{\Delta E_{\rm trans}}{\Delta E_{\rm ex}} = \frac{\nabla' - \nabla}{\nabla_{\rm ad} - \nabla'} = \frac{D_{\rm mix}}{2(K + D_h)} \left(\frac{d}{l}\right)^2 = \frac{\rm Pe}{6}. \quad (1)$$

The quantity Γ measures the deficit or excess of energy transported by rising or sinking turbulent elements $\Delta E_{\rm trans}$ with respect to the energy $\Delta E_{\rm ex}$ the elements gain or lose through the radiative (K) plus turbulent (D_h) heat exchange with the surroundings.

For an ideal gas, the square of the Brunt-Väisälä (buoyancy) frequency is

$$N^2 = \frac{g}{H_P}(\nabla' - \nabla + \nabla_\mu - \nabla'_\mu). \quad (2)$$

This equation takes into account that horizontal diffusion (molecular plus turbulent) may change the mean molecular weight of the fluid element μ' during its motion, so that $\nabla'_\mu \neq 0$. The convective instability sets in when N^2 becomes negative. By analogy with equation (1) and following Talon & Zahn (1997), we introduce a μ-transport efficiency

$$\Gamma_\mu = -\frac{\nabla'_\mu - \nabla_\mu}{\nabla'_\mu} = \frac{3D_{\rm mix}}{2(\nu_{\rm mol} + D_h)} \left(\frac{d}{l}\right)^2, \quad (3)$$

where $\nu_{\rm mol}$ is the molecular diffusivity. Supplementing the radiation luminosity with a contribution to heat transport by convection in the same manner as Maeder (1995) dealt with shear mixing, we obtain the following relation between ∇, $\nabla_{\rm rad}$, and $\nabla_{\rm ad}$,

$$\nabla = \frac{\nabla_{\rm rad} + 6\left[\Gamma^2/(\Gamma+1)\right][(K + D_h)/K](l/d)^2 \nabla_{\rm ad}}{1 + 6\left[\Gamma^2/(\Gamma+1)\right][(K + D_h)/K](l/d)^2}. \quad (4)$$

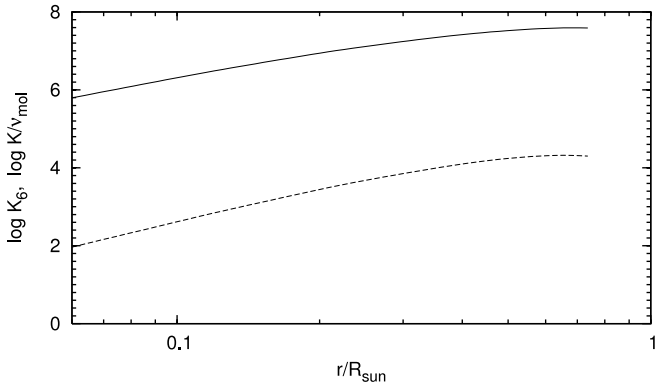

FIG. 2.—Profiles of the ratio of the thermal and molecular diffusivity (*solid curve*) and of the quantity $K_6 \equiv K/10^6$ cm^2 s^{-1} (*dashed curve*) in the radiative zone of our 0.83 $M_\odot$ bump luminosity model.

Combining equations (1)–(4), the instability condition $N^2 < 0$ can be transformed into

$$-\nabla_\mu > \left(\frac{\Gamma_\mu + 1}{\Gamma_\mu}\right) \frac{\Gamma}{1 + \Gamma + 6\Gamma^2[(K + D_h)/K](l/d)^2} (\nabla_{\rm ad} - \nabla_{\rm rad}). \quad (5)$$

2.1. *The Adiabatic Limit*

In the case of $\Gamma \gg 1$, equations (1) and (4) give $\nabla' \approx \nabla \approx \nabla_{\rm ad}$, which we call "the adiabatic limit." From equations (1) and (3) it follows that

$$\Gamma_\mu = 3\frac{K + D_h}{\nu_{\rm mol} + D_h}\Gamma, \quad (6)$$

hence $\Gamma_\mu \gg 1$ as soon as $\Gamma \gg 1$ because $\nu_{\rm mol} \ll K$ (Fig. 2). Using these constraints, the condition (5) is transformed to

$$D_{\rm mix} > \frac{1}{3} K \frac{\nabla_{\rm ad} - \nabla_{\rm rad}}{|\nabla_\mu|} \gg K. \quad (7)$$

Radial displacements $l \sim 10^8$ cm of fluid elements with velocities of order 5×10^4 cm s^{-1} observed by EDL06 in their 3D red giant model above the major H-burning shell correspond to a diffusion coefficient $D_{\rm mix} \sim \frac{1}{3} vl \sim 2 \times 10^{12}$ cm^2 s$^{-1} \gg K$. The same or even higher order of magnitude estimate can be obtained if we calculate $D_{\rm mix} \sim vH_P$, where $v^2 \sim gH_P\Delta\mu/\mu$, as proposed by EDL06 (see § 4). So, it appears that the ^{3}He-driven mixing in the 3D red giant model of EDL06 somehow wound up in the metastable adiabatic limit. We explore the consequences of such a rapid mixing process for both surface abundances and the thermal structure in § 4.

2.2. *The Radiative Limit*

Let us now consider a situation when $\Gamma(l/d)^2 \ll 1$. This also means that $\Gamma \ll 1$, because we have assumed that $d \leq l$. In this case, equations (1) and (4) give $\nabla' \approx \nabla \approx \nabla_{\rm rad}$; therefore, we refer to it as "the radiative limit." Given that in equation (6) the ratio $K/\nu_{\rm mol} \gg 1$ (solid curve in Fig. 2), the assumption that $\Gamma \ll 1$ does not automatically lead to $\Gamma_\mu < 1$ unless $D_h \gtrsim K$. Hence, we have to consider the cases of $\Gamma_\mu \gg 1$ and $\Gamma_\mu < 1$ separately.

1. In the radiative limit ($\Gamma \ll 1$), values of $\Gamma_\mu \gg 1$ can be met only if $D_h \ll K$. Using these constraints, the condition (5) is simplified to

$$D_{\rm mix} < \frac{2K}{\nabla_{\rm ad} - \nabla_{\rm rad}} |\nabla_\mu| \left(\frac{l}{d}\right)^2. \quad (8)$$

The right-hand side of equation (8) adequately reproduces both the diffusion coefficient for thermohaline convection derived by Kippenhahn et al. (1980),

$$D_{\rm Kipp} = \frac{3K}{\nabla_{\rm ad} - \nabla_{\rm rad}} |\nabla_\mu|, \quad (9)$$

who argued that l should be of order d, and the rate of mixing by elongated narrow "fingers" ($l > d$) advocated by Ulrich (1972),

$$D_{\rm Ulrich} = \frac{8}{3}\pi^2 \frac{K}{\nabla_{\rm ad} - \nabla_{\rm rad}} |\nabla_\mu| \left(\frac{l}{d}\right)^2. \quad (10)$$

Thus, in the radiative limit with $D_h \ll K$ we can readily identify mixing with thermohaline convection. Substituting expressions (9)–(10) in place of $D_{\rm mix}$, we find that, for thermohaline convection driven by the ^{3}He burning,

$$\Gamma \approx \frac{vl}{6K}\left(\frac{d}{l}\right)^2 \approx \frac{D_{\rm mix}}{2K}\left(\frac{d}{l}\right)^2 \approx \frac{|\nabla_\mu|}{\nabla_{\rm ad} - \nabla_{\rm rad}} \ll 1, \quad (11)$$

as we assumed.

2. If D_h is not negligibly small compared with K, then we sure have $D_h \gg \nu_{\rm mol}$, and relation (6) can be rewritten as

$$\Gamma_\mu = 3\frac{K + D_h}{D_h}\Gamma. \quad (12)$$

For $\Gamma_\mu < 1$, the condition (5) takes the form (compare it with condition [5] from Vauclair 2004)

$$\frac{|\nabla_\mu|}{\nabla_{\rm ad} - \nabla_{\rm rad}} > \frac{1}{3}\frac{D_h}{K + D_h}. \quad (13)$$

In the radiative zone of an LM-RGB star, the left-hand side of equation (13) is of order 10^{-3} at most. A profile of the quantity K in the radiative zone of our 0.83 $M_\odot$ bump luminosity model is plotted with a dashed curve in Fig. 2. Given that $K \lesssim 10^9$ cm^2 s^{-1} for $r \lesssim 0.1\ R_\odot$ and comparing the ratio D_h/K with the number 10^{-3}, we conclude that the horizontal turbulent diffusion with $D_h \gtrsim 10^6$ cm^2 s^{-1} may hinder the development of convective instability. It is interesting that such values of D_h have been found by Palacios et al. (2006) in their low-metallicity 0.85 $M_\odot$ bump luminosity model even for the less favorable case of solid-body rotation of the convective envelope. For the case of differential rotation of the convective envelope, which is suggested by observed fast rotation of horizontal branch stars, they have obtained $D_h \gtrsim 10^7$ cm^2 s^{-1}. For such large values of D_h, the right-hand side of equation (13) exceeds the expression on the left-hand side at least for $r \lesssim 0.1\ R_\odot$ (Fig. 2); therefore, the convection (thermohaline mixing) will probably be suppressed there.

3. ULRICH'S SOLUTION IN THE PRESENCE OF HORIZONTAL TURBULENT DIFFUSION

In this section we demonstrate that Ulrich (1972) could have come to a conclusion about the suppression of thermohaline convection by the strong horizontal turbulent diffusion similar to that made by us (condition [13]) if he had included D_h in his equations. To do this, we start with the linearized equations of conservation of momentum, thermal energy, and chemical composition similar to those used by Ulrich (his eqs. [1]–[3]) but with the diffusion coefficient D_h taken into account,

$$2\frac{dv}{dt} = -\frac{\nu}{d^2}v - g\,\delta \ln T + g\,\delta \ln \mu, \quad (14)$$

$$\frac{d\delta \ln T}{dt} = \frac{(\nabla_{\rm ad} - \nabla_{\rm rad})}{H_P}v - \frac{(K + D_h)}{d^2}\delta \ln T, \quad (15)$$

$$\frac{d\delta \ln \mu}{dt} = -\frac{\nabla_\mu}{H_P}v - \frac{(\nu_{\rm mol} + D_h)}{d^2}\delta \ln \mu. \quad (16)$$

Here, $\nu = \nu_{\rm mol} + \nu_{\rm rad}$ is the total (molecular plus radiative) viscosity, $\delta \ln T = \ln T'(r) - \ln T(r)$, $\delta \ln \mu = \ln \mu'(r) - \ln \mu(r)$, and the other symbols have been defined above.

The characteristic polynomial for the linear system of ODEs (14)–(16) can be written in the following form,

$$\begin{aligned}&(\omega\tau_{\rm th})^3 + \left[1 + (\tau_{\rm th}/\tau_\nu) + (\tau_{\rm th}/\tau_\mu)\right](\omega\tau_{\rm th})^2 \\ &+ \left[(\tau_{\rm th}/\tau_\nu) + (\tau_{\rm th}/\tau_\nu)(\tau_{\rm th}/\tau_\mu) + (\tau_{\rm th}/\tau_\mu) + (\tau_{\rm th}^2 N^2)\right](\omega\tau_{\rm th}) \\ &+ \left[(\tau_{\rm th}/\tau_\nu)(\tau_{\rm th}/\tau_\mu) + (\tau_{\rm th}^2 N_\mu^2) + (\tau_{\rm th}/\tau_\mu)(\tau_{\rm th}^2 N_T^2)\right] = 0,\end{aligned} \quad (17)$$

where $\omega = 2\pi\tau_{\rm mix}^{-1}$ is the eigenfrequency of the stable ($\omega < 0$) or unstable ($\omega > 0$) mode, $N_T^2 = g(\nabla_{\rm ad} - \nabla_{\rm rad})H_P^{-1}$ and $N_\mu^2 = g\nabla_\mu H_P^{-1}$ are the squares of the T- and μ-components, respectively, of the Brunt-Väisälä frequency for the ideal gas, $N^2 = N_T^2 + N_\mu^2$, while $\tau_\nu = d^2/\nu$, $\tau_{\rm th} = d^2/(K + D_h)$, and $\tau_\mu = d^2/(\nu_{\rm mol} + D_h)$ denote the viscous, thermal, and horizontal diffusion timescales for the fluid element. Our equation (17) is equivalent to Ulrich's dispersion relation (10).

The only real root of the polynomial (17) is plotted as a function of (D_h/K) in Figure 3 for the ratio $d/H_P = 0.01$ and three different values of $N_\mu^2 = -10^{-7}$ (*solid line*), -10^{-6} (*short-dashed line*), and -10^{-8} (*long-dashed line*). The first value of N_μ^2 is close to the minimum one found in the region of the μ-gradient inversion produced by ^{3}He burning in a low-metallicity bump luminosity star with a mass $M \approx 0.8\ M_\odot$. The quantities $(\omega\tau_{\rm th})$ and (D_h/K) in Figure 3 have been scaled appropriately to reveal both our guessed functional dependence (10) and instability condition (13). At a fixed value of N_μ^2, our solutions for the ratio d/H_P varying from 0.01 down to 0.0001 coincide. From Figure 3, we conjecture that

$$D_{\rm mix} \sim \frac{l^2}{\tau_{\rm mix}} \sim \frac{l^2}{\tau_{\rm th}}(\omega\tau_{\rm th}) \sim K\frac{|N_\mu^2|}{N_T^2}\left(\frac{l}{d}\right)^2\left(1 - \frac{D_h}{K}\frac{N_T^2}{|N_\mu^2|}\right), \quad (18)$$

i.e. the thermohaline convective instability may develop ($\omega > 0$) only if $D_h < K|N_\mu^2|/N_T^2$. The latter condition is equivalent (ignoring factors of order unity) to equation (13) for $D_h < K$. If $D_h \ll K$, then we can neglect the term in the parentheses. In this case we obtain an expression for $D_{\rm mix}$ similar to Ulrich's original formula.

Note that an equation similar to equation (18) can be derived directly from the dispersion relation (17) in the same way that Ulrich used to estimate $D_{\rm mix}$ in equation (10). Following him, we ignore the viscosity and take advantage of the fact that the thermohaline mode is the slowest one ($\omega\tau_{\rm th} \sim \tau_{\rm th}/\tau_{\rm mix} \ll 1$).

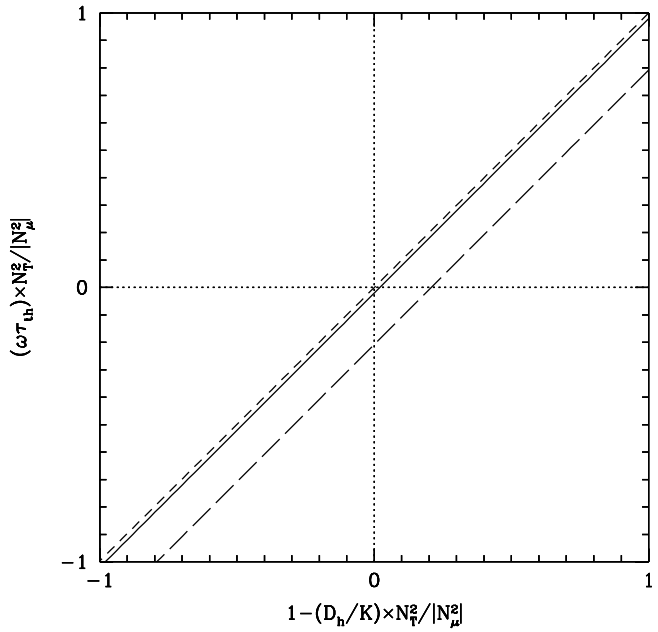

FIG. 3.—Solutions of the dispersion relation (17) as a function of the horizontal turbulent diffusion coefficient. Both the only real root ($\omega\tau_{\rm th}$) and the parameter (D_h/K) have been scaled appropriately to reveal the dependence (10) and the instability condition (13). Plotted are the solutions for the fluid element diameter $d = 0.01H_P$ and three values of $N_\mu^2 = -10^{-7}$ (this is a characteristic value for ^{3}He burning in low-metallicity bump luminosity stars with $M \approx 0.8\ M_\odot$; *solid line*), -10^{-6} (*short-dashed line*), and -10^{-8} (*long-dashed line*).

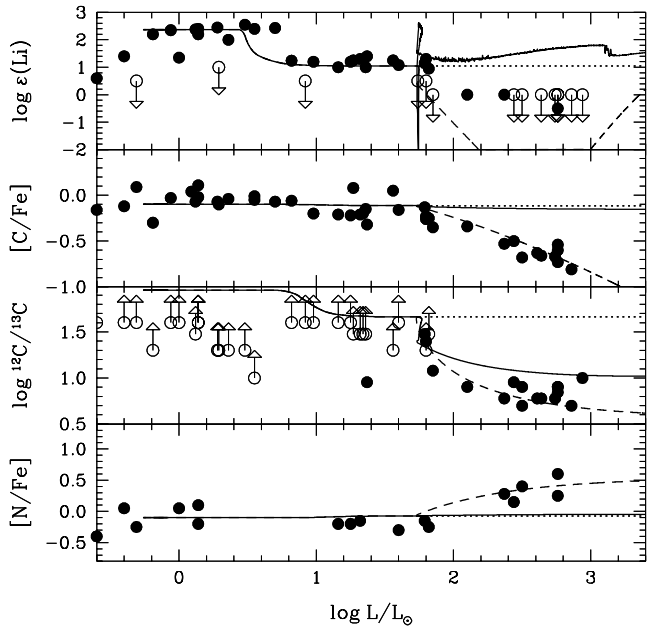

FIG. 4.—Comparison of the observational data from Gratton et al. (2000) for field metal-poor ($-2 \lesssim$ [Fe/H] $\lesssim -1$) low-mass stars (*circles*) with results of our computations of the evolution of the 0.83 $M_\odot$ star with the ^{3}He-driven mixing (*solid curves*, eqs. [20]) and extra mixing with the rate $D_{\rm mix} = 0.02K$ and depth $\Delta \log T = 0.19$ (*dashed curves*). Dotted lines show predictions of the standard theory. For further details, see text.

Therefore, we can neglect the quadratic and cubic terms in equation (17) as well as terms with τ_ν^{-1}. Taking into account that $N_T^2 \gg |N_\mu^2|$ and $N^2 \gg (\tau_{\rm th}\tau_\mu)^{-1}$, we finally obtain

$$D_{\rm mix} \sim (K + D_h)\frac{\left|N_\mu^2\right|}{N_T^2}\left(\frac{l}{d}\right)^2\left[1 - \frac{(\nu_{\rm mol} + D_h)}{(K + D_h)}\frac{N_T^2}{\left|N_\mu^2\right|}\right], \qquad (19)$$

which is reduced to equation (18) if $\nu_{\rm mol} < D_h < K$.

4. OBSERVATIONAL CONSTRAINTS ON THE EXTRA-MIXING RATE

The ^{3}He mechanism has a different underlying origin than rotational mixing, and it is therefore useful to reevaluate the global implications of its operation. This is especially true because we have identified two stable branches with very different timescales. We begin by establishing that a mixing process which occurs over too short of a timescale would have a dramatic impact on the thermal structure which contradicts the observational data. We also demonstrate that diffusion coefficients derived from empirical mixing estimates are consistent with the data.

We then critically examine whether thermohaline mixing is capable of reproducing the data, and the answer depends critically on the assumed geometry of the fluid elements (and the rate at which they can achieve thermal balance with their surroundings). However, we can also extend the same underlying mechanism to predict luminosity trends, behavior in other evolutionary states, and implications for interacting binaries. Definite predictions emerge, and we can identify both existing conflicts and topics which will require further calculation. In particular, we contend that the natural expectation would be for mixing that is shallower in temperature and weaker for bright giants than current data indicates. The predictions for other types of stars are fundamentally different, and in our view, the latter test will ultimately prove to be decisive.

4.1. *Rapid Mixing in the Adiabatic Limit*

The observed changes in the surface abundances of Li and C and in the ^{12}C/^{13}C ratio as a function of luminosity in LM-RGB stars (e.g., Charbonnel et al. 1998; Gratton et al. 2000) can be used to constrain the depth and rate of extra mixing in them. If $\Delta \log T$ is the difference between the logarithms of temperature at the base of the H-burning shell and at the maximum depth of extra mixing and $D_{\rm mix}$ is the diffusion coefficient, then as Denissenkov & VandenBerg (2003) have demonstrated, extra mixing in LM-RGB stars can be parameterized by any pair of correlated values within the close limits specified by $\Delta \log T \approx 0.19$ and $D_{\rm mix} \approx 4 \times 10^8$ cm^2 s^{-1} to $\Delta \log T \approx 0.22$ and $D_{\rm mix} \approx 8 \times 10^8$ cm^2 s^{-1}. However, that parameterization did not take into consideration the thermal response of the radiative zone to mixing.

In this paper we use a more consistent parametric prescription by letting $D_{\rm mix}$ be equal to a fixed fraction of K and allowing the temperature gradient in the radiative zone to be modified as prescribed by the mixing length theory relation (4). It is inspired by a similarity between equation (9) and the functional dependence of $D_{\rm mix}$ on K obtained for rotational shear mixing by Maeder & Meynet (1996).

We derive $\Gamma = 0.01$ for the mixing depth $\Delta \log T = 0.19$ constrained by Denissenkov & VandenBerg (2003), which results in the diffusion coefficient $D_{\rm mix} = 0.02K$ (assuming that $l \approx d$ and $D_h \ll K$ in eq. [1]). These models reproduce quite well the chemistry of LM-RGB stars above the bump luminosity (dashed curves in Fig. 4). They do not noticeably change our models' photometric behavior and evolutionary timescale near the bump luminosity compared to models without extra mixing. This is important because photometric observations of LM-RGB stars, in particular the absolute V-band magnitude of the luminosity

bump and the excess number of stars in the bump, agree with predictions of standard stellar evolution theory (e.g., Bjork & Chaboyer 2006). Our test computations have shown that the ratio of the gradients in equations (9)–(10) does not change much with radius and that it is roughly proportional to the abundance of ^{3}He left in the mixing zone.

On the other hand, already at $\Gamma = 0.4$ the bump luminosity zigzag gets so extended toward a lower luminosity (dashed curve in top panel in Fig. 1) and the model star spends so long of a time following it that this peculiar behavior would surely have been noticed in photometric studies, such as the counting of the number densities of stars as a function of luminosity on the RGBs of globular clusters. To be more specific, it takes about twice as long for the model star to make the extended zigzag as compared to the standard evolution. It should also be noted that the model of such a rapidly mixed star spends most of this time residing near the bottom of the zigzag, about 0.3 mag below the standard bump luminosity. Values of $\Gamma > 0.4$ would result in even more drastic changes. This behavior is similar to that of models of rapidly rotating RS CVn binaries found by Denissenkov et al. (2006) except that in the latter case the extended zigzag was produced by an increase of ∇ caused by the stars' rotational deformations.

The estimate of the turbulent velocity $v^2 \sim gH_P(\Delta\mu/\mu)$ for the ^{3}He-driven mixing used by EDL06 can be obtained from equation (2) if we put into it $\nabla' - \nabla = \nabla'_\mu = 0$. Indeed, in this case we can approximately consider that $v^2 \sim H_P^2|N^2| = gH_P|\nabla_\mu| = gH_P^2(d\ln\mu/dr) \sim gH_P(\Delta\mu/\mu)$, at least in the vicinity of the ^{3}He-burning shell where the mean molecular weight height scale is of order H_P (bottom panel in Fig. 1). Note that in the mixing length theory the approximations $\nabla' = \nabla$ and $\nabla'_\mu = 0$ are correct only in the limits of $\Gamma = \infty$ or $\Gamma = 0$, and $\Gamma_\mu = \infty$ (eqs. [1]–[4]).

Neglecting the influence of extra mixing on the radiative zone's thermal stratification, we have computed the evolution of our model also with the following diffusion coefficient,

$$D_{\rm mix} = \frac{1}{3} H_P v, \quad \text{where } v^2 = \frac{1}{8} gH_P|\nabla_\mu|. \tag{20}$$

The factor $\frac{1}{8}$ comes from the mixing length theory (Weiss et al. 2004, p. 387). The depth of this "^{3}He-driven" extra mixing has been determined by locating the minimum of μ above the H-burning shell. Outside of this point, μ increases with radius due to the ^{3}He burning and mixing. We think that our prescription is in line with that EDL06 had in mind. It should be noted that in our computations values of $D_{\rm mix}$ were determined at each time step using a current distribution of μ that was constantly modified by extra mixing. Characteristic values of $D_{\rm mix}$ obtained in this self-regulating way were of order 10^{12} cm^2 s^{-1}. Such fast extra mixing is known to produce large amounts of ^{7}Li via the Cameron-Fowler mechanism (e.g., Denissenkov & Weiss 2000; Denissenkov & Herwig 2004). This disagrees with the low (often undetectable) Li abundances in the majority of LM-RGB stars located above the bump luminosity (compare the solid curve above $\log L/L_\odot \approx 1.8$ with the observational data points in top panel in Fig. 4). In accordance with EDL06, we did find a modest decrease in the ^{12}C/^{13}C ratio. However, it is obvious that the observed evolutionary changes of the surface chemical composition of LM-RGB stars require a slightly deeper (in order to reproduce the C depletion) and much slower (in order to keep the Li abundance low) extra mixing than that advocated by EDL06. Besides, extra mixing with diffusion coefficients $D_{\rm mix} \gg K \sim 10^8$–$10^{10}$ cm^2 s^{-1} would bring the radiative zone to the quasi-adiabatic state (unless the fluid elements have fingerlike structures, which has not been reported by EDL06), which would cause the star to make a prolonged excursion below the bump luminosity in contradiction with observations. Therefore, we believe that the rapid mode originally invoked by EDL06 does not operate, but that mild mixing is indicated.

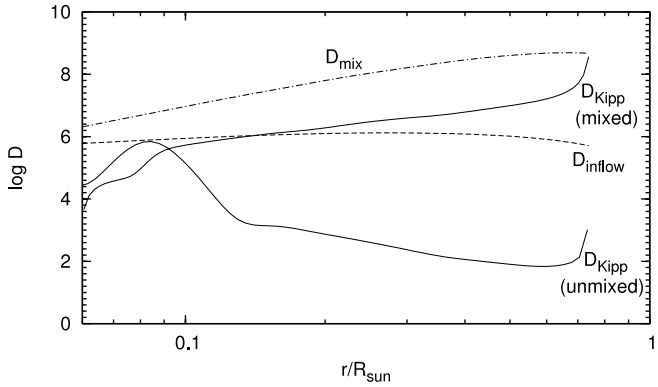

FIG. 5.— Characteristic diffusion coefficients. *Dot-dashed curve*: Empirical profile of $D_{\rm mix} = 0.02K$. *Dashed curve*: Minimum threshold profile $D_{\rm inflow} = |\dot{r}|H_P$ that any $D_{\rm mix}$ must exceed. *Bottom solid curve*: The $D_{\rm Kipp}$ (thermohaline convection, eq. [9]) profile in our unmixed bump luminosity model (a hump at $r \approx 0.08\ R_\odot$ is produced by a local increase of $|\nabla_\mu|$ in the ^{3}He-burning shell). *Top solid curve*: The $D_{\rm Kipp}$ profile in a model in which mixing with $D_{\rm mix} = 0.02K$ has spread out the μ-gradient inversion over the entire radiative zone.

4.2. *Mild Thermohaline Mixing in the Radiative Limit*

Because the ^{3}He-driven thermohaline convection is expected to work in the radiative limit, it is interesting to test if it is fast and deep enough to explain extra mixing in LM-RGB stars. In Figure 5 we illustrate characteristic diffusion coefficients. In order to produce mixing, a physical mechanism must operate over a timescale shorter than the inflow rate. The dot-dashed curve shows our empirically constrained diffusion coefficient $D_{\rm mix} = 0.02K$. For comparison, the dashed curve shows a minimum threshold diffusion coefficient $D_{\rm inflow} = |\dot{r}|H_P$, where $|\dot{r}|$ is a mass inflow rate of H-rich material that flows from the bottom of the convective envelope toward the H-burning shell (resembling a spherical accretion). The bottom solid curve shows a profile of the diffusion coefficient (9) in our unmixed bump luminosity model. Once mixing ensues, the μ-gradient inversion spreads out over the entire radiative zone above the ^{3}He-burning shell. The final state is illustrated with the top solid curve. We conclude that, in the prescription given by Kippenhahn et al. (1980), the thermohaline convection could marginally commence and mix a narrow region in the vicinity of the ^{3}He-burning shell (at $r \approx 0.08\ R_\odot$ in Fig. 5). However, the Kippenhahn et al. diffusion coefficient is only marginally large enough to trigger this process and is 2 orders of magnitude below the empirical value.

If we adopt the Ulrich prescription (10) with $l \approx 10d$, our diffusion coefficient is raised by a factor of 10^2 and the mechanism may be viable. This is the approach advocated by Charbonnel & Zahn (2007; incidentally, their paper was posted on astro-ph on the same day when we submitted the first version of our paper).

Unfortunately, Charbonnel & Zahn (2007) do not explain how they have chosen the depth of mixing. We find that the depth corresponding to a minimum on the μ-profile (solid vertical line segments in Fig. 6) is not sufficient to produce the observed C depletion (second panel from the top in Fig. 4). An overshooting on a length scale of order H_P could do it (dotted vertical line segments in Fig. 6 are placed at a distance H_P below

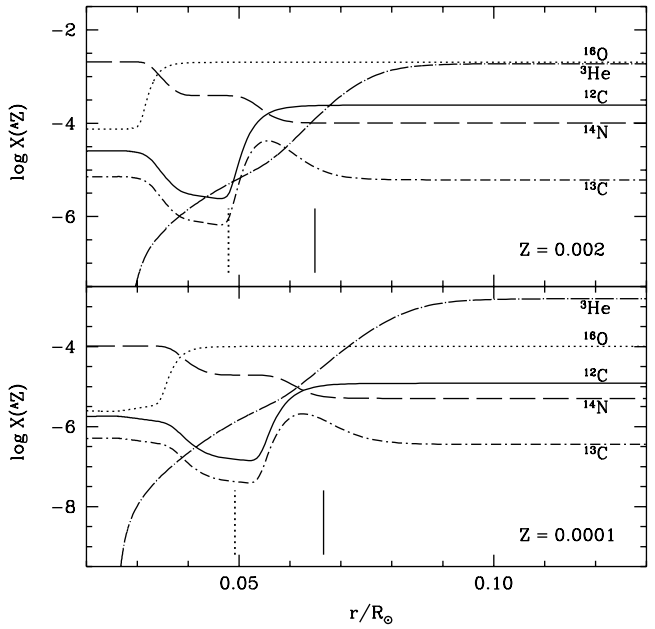

FIG. 6.—Profiles of the mass fractions of ^{3}He and CNO elements in the vicinity of the H-burning shell in 0.83 $M_\odot$ bump luminosity models with the heavy-element mass fractions $Z = 0.002$ and 0.0001. Vertical solid line segments show locations of the minimum on the μ-profile. Dotted line segments are placed one pressure scale height below $\mu_{\rm min}$. Without overshooting, the depth of the ^{3}He-driven thermohaline convection would be at the locations of the solid segments. There would be no evolutionary C depletion in this case, contrary to observations.

$\mu_{\rm min}$), but then thermohaline "fingers" would have to penetrate down a region of higher μ where they should experience a strong breaking. It should also be noted that the penetration of a region with negative $d\mu/dr$ below $\mu_{\rm min}$ would reduce the average mixing rate by decreasing the slope of the positive $d\mu/dr$ in the mixing zone. Given these uncertainties that cannot be resolved from first principles but instead require empirical calibrations and/or higher resolution 3D hydrodynamic simulations, we postpone the use of equation (10) to our future paper.

5. CONCLUDING REMARKS

In this paper we have shown that the ^{3}He burning in the radiative zone of an LM-RGB star may drive convective fluid motions provided that their heat transport efficiency is either very high (the adiabatic limit) or extremely low (the radiative limit). Confirming the conclusions made by Charbonnel & Zahn (2007), we identify the mixing in the radiative limit with thermohaline convection and we note that this convection would have a sufficiently high rate to explain the observed mixing pattern in LM-RGB stars only if fluid elements could travel over length scales exceeding their diameters by a factor of 10 or more. However, we also find that thermohaline convection may be suppressed by horizontal turbulence if its associated diffusivity $D_h \gtrsim 3K|\nabla_\mu|/(\nabla_{\rm ad} - \nabla_{\rm rad})$. Such values of D_h for rotation-induced horizontal turbulence have been obtained by Palacios et al. (2006), who used a prescription for estimating D_h proposed by Mathis et al. (2004). Although this prescription may be considered as a very primitive approximation to a complex physical phenomenon, a similar heuristic approach has been used to successfully model mixing and angular momentum transport in radiative zones of massive MS stars (e.g., Talon & Zahn 1997; Talon et al. 1997; Maeder 2003). Of course, we recognize that rigorous 3D hydrodynamic simulations have yet to be done to support or refute these heuristic models. In addition to the theoretical issues above, there are significant empirical challenges for an explanation that relies solely on thermohaline convection. The same physics should consistently be applied to other phases of evolution or situations where μ-inversions occur.

If extra mixing in RGB stars is really driven by ^{3}He burning, then it should die out by the end of the RGB evolution because of the ^{3}He exhaustion. In this case, the ^{3}He-driven extra mixing could not resume working in the same stars on the asymptotic giant branch (AGB). So, we would expect the absence of observational signatures of extra mixing in low-mass ($M \lesssim 2\ M_\odot$) AGB stars unless the mixing in them is of a different nature. However, given the similarities in their depth and in the structure of radiative zone where they operate, it is unlikely that the RGB and AGB mixing have different physical mechanisms. Contrary to this prediction, there are observational data indicating the presence or necessity of operation of extra mixing in these stars (e.g., Nollett et al. 2003; Masseron et al. 2006). Moreover, to comply with observations, the AGB mixing has to penetrate close enough to the H-burning shell to dredge up material processed in the CN-cycle, like in RGB stars, mimicking the convective hot bottom burning that occurs in more massive AGB stars.

Stancliffe et al. (2007) have used the Kippenhahn et al. prescription (9) to model thermohaline mixing in a metal-poor low-mass MS star accreting wind material from its AGB binary companion enriched in He and C. Such accretion is believed to be the primary process responsible for the formation of the so-called carbon-enhanced metal-poor (CEMP) stars. They have found that thermohaline convection mixes almost 90% of the star within about 10^9 yr after the accretion. On the other hand, the RGB mixing pattern can be reproduced only if the diffusion coefficient given by equation (9) is increased by a factor of 10^2–10^3 (Charbonnel & Zahn 2007; also see our Fig. 5). In this case, thermohaline mixing in CEMP MS stars would dilute the accreted material on a much shorter timescale of order 10^6–10^7 yr. Unless most of the CEMP stars accreted substantial fractions of their initial masses, their rather high frequency $f_{\rm CEMP} \gtrsim 20\%$ among very metal-poor stars (e.g., Lucatello et al. 2006) would look surprising. Furthermore, both Lucatello et al. (2006) and Aoki et al. (2007) have found anticorrelations between [C/H] (and [(C+N)/H]) and luminosity for Ba-enhanced CEMP stars spanning over 3 orders of magnitude in L that they interpreted as evidence of dilution of the envelope material in the accreting companion. Thermohaline convection on a timescale of order 10^6–10^7 yr would mix the CEMP MS stars almost instantaneously and well before their luminosity would begin to increase due to the core H exhaustion. In that case, the mentioned anticorrelations could not have appeared. Also note that even on the lower RGB, Ba-enhanced CEMP stars have quite low carbon isotopic ratios (^{12}C/^{13}C < 20; Ryan et al. 2005) in a striking contrast with the values of ^{12}C/^{13}C $\gg 1000$ that the low-mass AGB stars are predicted to return to the interstellar medium (Herwig 2004). Extra mixing (in the low-mass AGB stars) could easily resolve this discrepancy.

The problem of mixing in CEMP MS and RGB stars has recently been addressed by Denissenkov & Pinsonneault (2008). Particularly, they have shown that the first dredge-up dilution of CN enrichment in CEMP stars relative to their MS precursors is indeed a plausible explanation of the observed anticorrelation of [N/Fe] with $\log L/L_\odot$ and that it contradicts models that rely on efficient thermohaline mixing induced by small μ-gradients in red giants. This result has independently been confirmed by Aoki et al. (2008). The suppression of thermohaline convection by rotationally driven horizontal turbulence may explain its reduced efficiency in MS CEMP stars.

Another potentially serious problem for the ^{3}He-driven thermohaline convection could be to explain available observational evidence of enhanced extra mixing in LM-RGB stars. First, observations show that in some globular clusters the anticorrelated abundance variations of C and N in red giants become larger when stars approach the RGB tip. Moreover, extremely large values of the N abundance in some of these stars indicate the dredge-up of material in which not only C but also a fraction of O has been converted into N (Smith et al. 2005a). Second, at least in the globular cluster M13, the relative number of upper RGB stars with the O-Na anticorrelation increases with luminosity (Johnson et al. 2005). Third, Denissenkov et al. (2006) have shown that the ^{19}F abundance variations found in bright red giants of the globular cluster M4 by Smith et al. (2005b) may also require the extra mixing in them to operate much faster and somewhat deeper than in LM-RGB stars immediately above the bump luminosity. It is difficult to interpret these data by the ^{3}He-driven mixing, because its efficiency should decline toward the RGB tip in proportion as ^{3}He gets depleted. Unfortunately, the question of evolutionary Na, O, and ^{19}F abundance variations in globular cluster RGB stars is still a matter of debate from the observational point of view. Therefore, we consider them as a potential rather than a real problem for the ^{3}He thermohaline convection.

A similar problem is encountered when one tries to understand the phenomenon of Li-rich giants. There are convincing arguments that high-Li abundances in these LM-RGB stars are produced via the Cameron-Fowler mechanism that also requires enhanced extra mixing with $D_{\rm mix} \sim 10^{10}$–10^{11} cm^2 s^{-1} (Denissenkov & Weiss 2000; Denissenkov & Herwig 2004). It should be noted that most of the Li-rich giants are located above the bump luminosity (Charbonnel & Balachandran 2000). Besides, their proportion among rapid rotators ($v \sin i \geq 8$ km s^{-1}) is $\sim$50%, which is considerably larger than the $\sim$2% of Li-rich stars among the much more common slowly rotating ($v \sin i \lesssim 1$ km s^{-1}) K-giants (Drake et al. 2002). It is not clear why the ^{3}He-driven mixing would be enhanced in fast rotators. Oppositely, Canuto (1999) argues that a larger shear due to differential rotation should decrease the efficiency of mixing by thermohaline convection. A larger shear would also intensify horizontal turbulence, thus hindering thermohaline convection even more strongly. So, the Li-rich giants seem to support the hypothesis of rotation-induced mixing rather than that of thermohaline mixing. This may not necessarily be rotational shear mixing that has already been criticized. Instead, rotation may deposit its kinetic energy to mixing less directly, e.g., through generation of buoyant magnetic flux tubes (Busso et al. 2007).

For the adiabatic limit, the predicted evolutionary changes of the surface composition of LM-RGB stars disagree with observational data. Besides, high Γ values would bring the radiative zone to the quasi-adiabatic state which would result in photometric behavior of the RGB star inconsistent with the observed one.

In the vicinity of $\mu_{\rm min}$, our empirically constrained diffusion coefficient has values of order $D_{\rm mix} \sim 10^6$–10^7 cm^2 s^{-1} (dot-dashed curve in Fig. 5). If we assume that in real LM-RGB stars extra mixing is produced by thermohaline convection whose fluid elements have a ratio of $l/d \sim 10$, where l does not exceed the local pressure scale height $H_P \sim 0.02\ R_\odot$, then we can estimate the elements' characteristic velocities $v \approx 3D_{\rm mix}/l \sim 2 \times 10^{-3}(H_P/l)$–$2 \times 10^{-2}(H_P/l)$ cm s^{-1}. EDL06 have found velocities of order 5×10^4 cm s^{-1} in their 3D red giant model. Those would correspond to fluid elements with diameters from 6 to 60 cm! Interestingly, such small fluid elements would actually be optically thin, because the photon mean free path is $\sim$1 cm in this environment. However, we do not believe that EDL06 could resolve such small fingerlike structures. As we mentioned, they have reported fluid element displacements of order $l \sim 10^8$ cm. Given the discussed inconsistencies in modeling extra mixing in LM-RGB stars with the ^{3}He-driven convection, we conclude that a different mechanism is worth searching for. It is also obvious that higher resolution 3D hydrodynamic simulations of the ^{3}He-driven mixing are needed to understand what EDL06 have actually witnessed. In particular, we quote here an issue raised by the referee, who seems to be an expert in the field. "The EDL06 calculations had no mechanism to simulate the turbulent cascade on scales smaller than the zoning (a sub–grid scale model, such as an eddy viscosity treatment), and yet, the calculations did not numerically blow up. To me this says that the finite-difference expressions of the Djehuty code are themselves quite diffusive. Thus, I am surprised that this incredibly small mean molecular weight inversion could generate significant motion without being squelched by the numerical diffusion. My conclusion is that there are some serious issues that must be addressed about the numerical behavior of the 3D calculations."

We thank the anonymous referee for useful comments and suggestions that helped us to improve the manuscript. We acknowledge support from the NASA grant NNG 05-GG20G.

REFERENCES

Aoki, W., Beers, T. C., Christlieb, N., Norris, J. E., Ryan, S. G., & Tsangarides, S. 2007, ApJ, 655, 492
Aoki, W., et al. 2008, ApJ, 678, 1351
Bania, T. M., Rood, R. T., & Balser, D. S. 2002, Nature, 415, 54
Bellman, S., Briley, M. M., Smith, G. H., & Claver, C. F. 2001, PASP, 113, 326
Bjork, S. R., & Chaboyer, B. 2006, ApJ, 641, 1102
Busso, M., Wasserburg, G. J., Nollett, K. M., & Calandra, A. 2007, ApJ, 671, 802
Canuto, V. M. 1999, ApJ, 524, 311
Chaboyer, B., & Zahn, J.-P. 1992, A&A, 253, 173
Chanamé, J., Pinsonneault, M., & Terndrup, D. M. 2005, ApJ, 631, 540
Charbonnel, C. 1995, ApJ, 453, L41
Charbonnel, C., & Balachandran, S. C. 2000, A&A, 359, 563
Charbonnel, C., Brown, J. A., & Wallerstein, G. 1998, A&A, 332, 204
Charbonnel, C., & Zahn, J.-P. 2007, A&A, 467, L15
Dearborn, D. S. P., Lattanzio, J. C., & Eggleton, P. P. 2006, ApJ, 639, 405
Denissenkov, P. A., Chaboyer, B., & Li, K. 2006, ApJ, 641, 1087
Denissenkov, P. A., & Herwig, F. 2004, ApJ, 612, 1081
Denissenkov, P. A., & Pinsonneault, M. 2008, ApJ, 679, 1541
Denissenkov, P. A., Pinsonneault, M., & Terndrup, D. M. 2006, ApJ, 651, 438
Denissenkov, P. A., & VandenBerg, D. A. 2003, ApJ, 593, 509
Denissenkov, P. A., & Weiss, A. 2000, A&A, 358, L49
Drake, N. A., de la Reza, R., da Silva, L., & Lambert, D. L. 2002, AJ, 123, 2703
Eggleton, P. P., Dearborn, D. S. P., & Lattanzio, J. C. 2006, Science, 314, 1580 (EDL06)
———. 2007, in IAU Symp. 239, Convection in Astrophysics, ed. F. Kupka, I. Roxburgh, & K. Chan (Cambridge: Cambridge Univ. Press), 286
Gilroy, K. K., & Brown, J. A. 1991, ApJ, 371, 578
Gratton, R. G., Sneden, C., Carretta, E., & Bragaglia, A. 2000, A&A, 354, 169
Grundahl, F., Briley, M., Nissen, P. E., & Feltzing, S. 2002, A&A, 385, L14
Herwig, F. 2004, ApJS, 155, 651
Hogan, G. J. 1995, ApJ, 441, L17
Johnson, C. I., Kraft, R. P., Pilachowski, C. A., Sneden, C., Ivans, I. I., & Benman, G. 2005, PASP, 117, 1308
Keller, L. D., Pilachowski, C. A., & Sneden, C. 2001, AJ, 122, 2554
Kippenhahn, R., Ruschenplatt, G., & Thomas, H.-C. 1980, A&A, 91, 175
Lucatello, S., Beers, T. C., Christlieb, N., Barklem, P. S., Rossi, S., Marsteller, B., Sivarani, T., & Lee, Y. S. 2006, ApJ, 652, L37
Maeder, A. 1995, A&A, 299, 84

Maeder, A. 2003, A&A, 399, 263
Maeder, A., & Meynet, G. 1996, A&A, 313, 140
Masseron, T., et al. 2006, A&A, 455, 1059
Mathis, S., Palacios, A., & Zahn, J.-P. 2004, A&A, 425, 243
Nollett, K.-M., Busso, M., & Wasserburg, G. J. 2003, ApJ, 582, 1036
Palacios, A., Charbonnel, C., Talon, S., & Siess, L. 2006, A&A, 453, 261
Rood, R. T., Bania, T. M., & Wilson, T. L. 1984, ApJ, 280, 629
Ryan, S. G., Aoki, W., Norris, J. E., & Beers, T. C. 2005, ApJ, 635, 349
Shetrone, M. D. 2003, ApJ, 585, L45
Smith, G. H., & Briley, M. M. 2006, PASP, 118, 740
Smith, G. H., Briley, M. M., & Harbeck, D. 2005a, AJ, 129, 1589
Smith, G. H., & Martell, S. L. 2003, PASP, 115, 1211
Smith, V. V., Cunha, K., Ivans, I. I., Lattanzio, J. C., Campbell, S., & Hinkle, K. H. 2005b, ApJ, 633, 392
Spite, M., et al. 2006, A&A, 455, 291
Stancliffe, R. J., Glebbeek, E., Izzard, R. G., & Pols, O. R. 2007, A&A, 464, L57
Sweigart, A. V., & Mengel, J. G. 1979, ApJ, 229, 624
Talon, S., & Zahn, J.-P. 1997, A&A, 317, 749
Talon, S., Zahn, J.-P., Maeder, A., & Meynet, G. 1997, A&A, 322, 209
Tosi, M. 1998, Space Sci. Rev., 84, 207
Ulrich, R. K. 1972, ApJ, 172, 165
Vangioni-Flam, E., Olive, K. A., Fields, B. D., & Cassé, M. 2003, ApJ, 585, 611
Vauclair, S. 2004, ApJ, 605, 874
Weiss, A., Hillebrandt, W., Thomas, H.-C., & Ritter, H. 2004, Cox & Giuli's Principles of Stellar Structure (2nd ed.; Cambridge: Cambridge Scientific)
Weiss, A., Wagenhuber, J., & Denissenkov, P. A. 1996, A&A, 313, 581
Zahn, J.-P. 1992, A&A, 265, 115